ISBN: 978-3-95450-184-7 doi:10.18429/JACoW-IPAC2018-THYGBF1

HIGH POWER BEAM OPERATION OF THE J-PARC RCS AND MR*

Y. Sato# for the J-PARC Accelerator Group, J-PARC center,
KEK&JAEA, 319-1195 Tokai, Naka, Ibaraki, Japan

Abstract

This presents the most recent status of improving the J-PARC main ring (MR) beam operation together with the rapid cycling synchrotron (RCS) effort. The RCS has optimized the beam performance for the MR injection as well as the muon and neutron targets, where each requires different emittance and beam halo size. The MR has two extraction modes; fast extraction (FX) for the long baseline neutrino oscillation experiment, T2K, and slow extraction (SX) for experiments in the hadron experimental facility. At present, achieved beam intensities are 2.56×10^{14} protons per pulse (ppp) with cycle time 2.48 s (495 kW) in the FX mode, and 5.5×10^{13} ppp with cycle time 5.20 s (51 kW) in the SX mode. For the FX operation, recent improvements are settings of new betatron tune, corrections of resonances near the betatron tune, and adopting 2nd harmonic RF voltage to reduce space charge effect. Beam instabilities have been suppressed with controlling chromaticity correction and transverse feedback systems. For the SX mode, a dynamic bump scheme for reducing extracted beam loss is successfully adopted. A high extraction efficiency of 99.5 % is achieved at 51 kW user operation.

INTRODUCTION

The Japan Proton Accelerator Research Complex (J-PARC) consists of the high intensity proton accelerators and the experimental facilities. The accelerators are the 400-MeV linear accelerator, the 3-GeV rapid cycling synchrotrons (RCS) and the 30-GeV main ring (MR) [1]. The RCS is a high power pulsed proton driver aiming 1 MW [2]. The RCS provides 3 GeV protons in 25 Hz to the materials and life science experimental facility (MLF) mostly and to the MR only four pulses every 2.48 s or 5.20 s by switching the beam destination pulse by pulse. The RCS operation needs to satisfy the different requirements of the beam properties for the MLF and the MR, and to keep good compatibility between them. The MR has two operational modes. One is with fast extraction to the neutrino experimental facility in 2.48 s cycle, and another is with slow extraction to the hadron experimental facility in 5.20 s cycle. In this paper, our recent commissioning of high intensity operation in the RCS and the MR are presented.

THE RCS OPERATION

The RCS provides high power beams to the MLF and the MR by switching the destinations pulse by pulse. Each destination requires different beam properties. Therefore, in the RCS, the injection bump, RF voltage, steering magnets, sextupoles and the power supplies of the quadrupole correctors can be switched pulse by pulse. A pulse-by-pulse switching of painting emittance, chromaticity and betatron tune enabled well-compatibility of different requirements from the MLF and the MR, keeping beam loss within acceptable levels [3, 4].

For the MLF

1 MW beam acceleration was achieved successfully [2]. Manipulating tune and chromaticity, and recovering super-periodic-condition, the transverse painting area was successfully expanded to 200π mm mrad [5]. This large painting enables reducing a foil-scattering beam loss during the injection, mitigating a major beam loss induced by space charge effect, and forming a wide-emittance beam with less charge density, which is required from the MLF to mitigate a shockwave on the neutron target. To change injection painting scheme from correlated painting to anti-correlated painting reduced the beam loss by a quarter [2]. Through the experiment and the simulation study, a new operating point was adopted also, and the beam loss was reduced by half [4].

For the MR

Low emittance beam with less beam halo is required in the MR, because its physical aperture is much smaller than the MLF. A small injection painting with 50π mm mrad is required, and tune and chromaticity are optimized to achieve the low emittance [4]. Based on simulations, step-by-step parameter optimizations were performed from ID1 to ID4 in Table 1. Figure 1 shows the measured extraction emittances for ID1 - 4, and the vertical emittance in ID4 was half of the one in ID1. Simulation predicted these emittance features well. Figure 2 shows the RCS tune during acceleration for the MLF and the MR. The tune for the MR is Set C of ID4 in Table 1. To manipulate tune, both of main quadrupoles and pulsed quadrupole correctors are used, and the pulsed quadrupole correctors realize a pulse-by-pulse switching of optimal tunes for the MLF and the MR [4].

Table 1: Operational parameter sets tested, where IDs show the identification number of each parameter set. The betatron tune of Set C was variated by adding 6 quadrupole-correctors, while Set A and Set B are manipulated only with main quadrupoles.

	ID1	ID2	ID3	ID4
Painting area (mm mrad)	51π	51π	51π	51π
Sextupole field	Off	Bipolar	Bipolar	Bipolar
Betatron tune	Set A	Set A	Set B	Set C

yoichi.sato@j-parc.jp

ISBN: 978-3-95450-184-7 doi:10.18429/JACoW-IPAC2018-THYGBF1

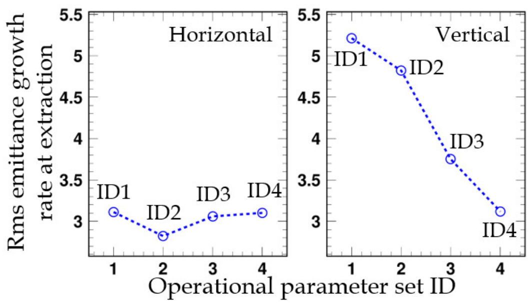

Figure 1: Rms emittance growth at extraction (ratio of normalized rms beam emittance to normalized rms painting emittance) measured with the parameter sets of ID1 - 4 in Table 1.

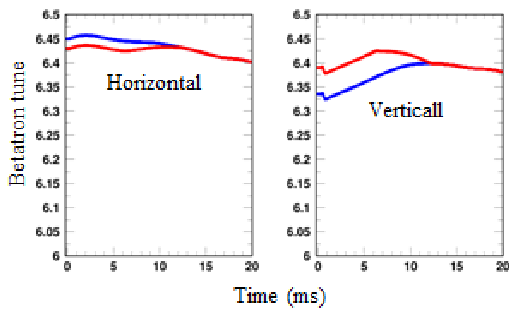

Figure 2: The RCS tune during acceleration. Left figure is for horizontal tune, and right is for vertical tune. Blue lines are for the MLF, and red lines are for the MR.

THE MR WITH FAST EXTRACTION

The MR FX achieved 420 kW in spring 2016, and 490 kW in present as stable user operation to the T2K (Fig. 3). In spring 2016 we changed our operation tune from (22.40, 20.75) to (21.35, 21.43) for larger tuneable area.

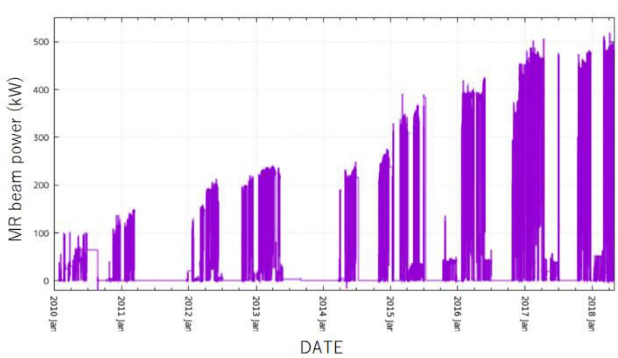

Figure 3: MR beam power trend. Maximum delivered power to user facilities are 490 kW with fast extraction and 51 kW with slow extraction.

Operation with Betatron Tune (21.35, 21.43)

The tune (22.40, 20.75) had been adopted from the beginning of our physics run till 2016. However, we encountered the effect of the half resonance $\nu_y = 20.50$ became too strong to increase beam power over 400 kW. We searched outside of the designed operation area through beam dynamics simulations, and the area around (21.35, 21.43) had wider area because we can expect longer distance to the major resonances [6]. In the high intensity operation at the new betatron tune, we need to minimize the effect of 2 third-order-resonances, $\nu_x + 2\nu_y = 64$ and $3\nu_x = 64$, besides the effect of $\nu_x = 21.0$ and $\nu_y = 21.5$ (see Fig. 4). We have re-optimized all tuning keys, most of which were already adopted in 2016 [7], to explore the new betatron tune, and adopted the tune in user operation.

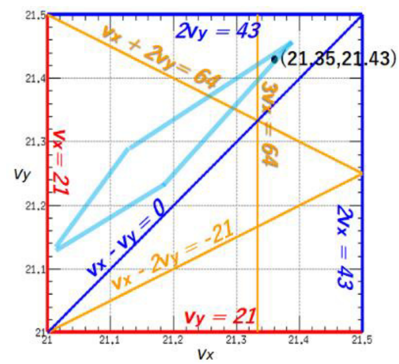

Figure 4: The betatron tune area of the MR with fast extraction since May 2016.

Beam Tuning Keys

The beam loss sources in the MR can be classified in:

1. Upstream beam quality from the RCS.
2. Physical aperture.
3. Emittance growth by betatron resonances.
4. Emittance growth by beam instability.

For the first source, we choose optimal conditions with measuring the 3-50BT profile monitors transversely [8], and beam losses in 3-50BT and the MR. To find the best conditions of the upstream, the rest conditions should be optimized in advance. The present RCS settings for the MR was discussed in the previous section. For the second source, beam optics and closed orbit are corrected to hold effective aperture. For the third source, we need to choose optimal operation point with managing space charge tune spread, chromatic tune spread, and resonance strength, which are mitigated with higher harmonic RF to control high bunching factor and increase longitudinal emittance, patterned chromatic correction by sextupoles, and enlarging dynamic aperture by correcting the leakage field of the FX septum magnets with trim coils of the nearest 3 quadrupoles and by correcting the second and third-order-resonances with trim coils of sextupoles and skew-quadrupoles. For the fourth source, controlling chromaticity correction and transverse feedback systems are adopted to suppress the instabilities. Octupole magnets are also used to compensate higher order effects. These tuning keys are related with multiple beam loss sources, especially tune spread and instability. Therefore, all keys should be tuned iteratively. To localize beam loss into the collimator section is also important. Most of all tuning keys above were arranged by 2016 [7] and they have been optimized respectively on the previous tune (22.40, 20.75) and the present tune (21.35, 21.43). Here we show specific tunings for the present tune.

ISBN: 978-3-95450-184-7 doi:10.18429/JACoW-IPAC2018-THYGBF1

Optics Correction

To use the present tune (21.35, 21.43) newly, we started to correct beam optics itself [9]. We made iterative correction with measuring the beam optics: tune, beta-function, phase, dispersion function and chromaticity. To compensate the leakage quadrupole fields from the fast extraction septum magnets, trim coils of the nearest three quadrupoles were optimized. The residual magnetic fields of the resonance quadrupoles, which are used in slow extraction operation, are degaussed in fast extraction operation.

RF Pattern

Combining fundamental harmonic RF and second harmonic RF cavities have been used to mitigate the space charge effect. The bunching factor is around 0.32 during the injection period. Longitudinal mismatch has been used on purpose by applying the second harmonic RF over 50% of the fundamental harmonic RF, to increase the bunching factor quickly within 5 ms after each injection. This approach causes higher bunching factor and larger longitudinal emittance simultaneously. The optimal balance has been determined by observing beam loss distribution and transverse instabilities, and considering chromatic tune spread, Landau damping effect and the longitudinal RF bucket size.

Compensation Kickers

The direction and kicking angle of the compensation kickers were optimized to the new tune, because they locate different place from the injection kickers which are the source of extra kick from their repulsing waves at the injection timings. This system enables the circulating bunch length stretched in 400-ns-long and allows our longitudinal tuning capability [10, 11].

Instability Suppression

The chromaticity is kept negative. It is -7 during injection and -3 in late acceleration with patterned sextupoles. Transverse-intra-bunch-feedback system is also used [12, 13]. These settings are relating with beam power and RF settings, and iterative tunings are necessary.

Resonance Corrections

The third order resonances of $\nu x + 2\nu y = 64$ and $3\nu x = 64$ have been corrected with trim coils of four sextupole magnets with the similar approaches for the previous tune, observing beam losses on each resonance line and identifying its driving factor by scanning the trim-sextupole fields. The differential resonance of $\nu x - \nu y = 0$ are corrected with using four skew quadrupoles. The trim sextupoles, skew-quadrupoles, and octupoles are optimized further with parameter scanning as a part of iterative high intensity tunings.

Tune Tracking for Bunch Train Tune Shift

Tune shift during injection period was observed in high intensity operation [14]. This effect depends on not only beam power but also number of bunches, and it is known as the bunch train tune shift, which comes from quadrupolar wake of non-circle beam pipe in the whole ring and provides opposite tune shifts horizontally and vertically [15]. The tune became (21.35, 21.44) for 2 bunches and (21.37, 21.42) for 8 bunches in 450 kW operation. This tune shift is not negligible in our high intensity operation, because of the limited area of optimal betatron tune. Figure 5 shows tune scan results of 2 bunch beam survival, keeping same tune during injection time (see Fig. 5). We optimize tune tracking with observing the betatron tune of the full intensity, to keep optimal operation tune during all period.

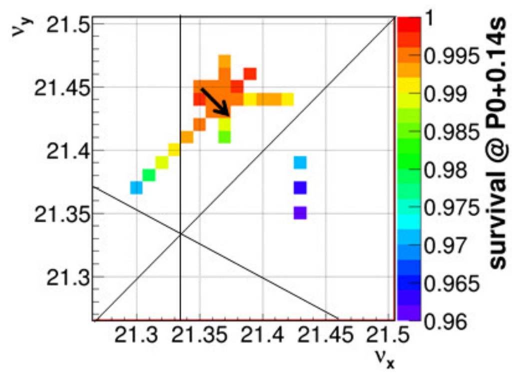

Figure 5: Tune scan results for the beam survival of 2 bunches of 450 kW equivalent beam during the injection period. Increasing number of bunches to 8 bunches, the tune shift (+0.02, -0.02) as in the black arrow.

Typical Operation of 490 kW

The MR achieved stable 490 kW user operation with fast extraction. There is no significant beam loss, but ~1% as total beam loss in the MR. As in Figures 6 and 7, beam losses in the MR are well localized at the collimator section in the first straight section and during injection period and low energy time. Residual activation also well localized, and one-foot dose is lower than 300 μSv/h in most of non-collimator section 4 hours after user operation. High intensity trial at 520 kW shows successful acceleration of 2.68 $\times 10^{14}$ ppp without significant beam loss. However, we need further tunings to achieve the same level of well beam loss localization as in the 490-kW operation. We are developing longitudinal feedback system, also.

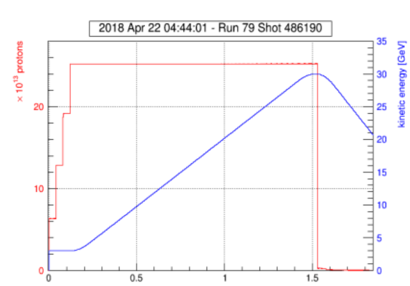

Figure 6: DCCT (red line) and kinetic energy pattern (blue line) of MR 490 kW with fast extraction in 2.48 s cycle. The total loss of MR is ~500 W, estimated from the DCCT response.

9th International Particle Accelerator Conference IPAC2018, Vancouver, BC, Canada JACoW Publishing
ISBN: 978-3-95450-184-7 doi:10.18429/JACoW-IPAC2018-THYGBF1

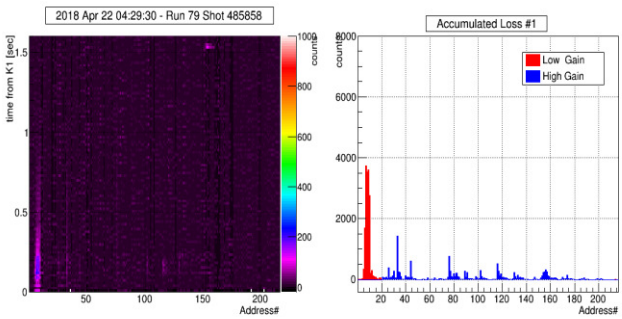

Figure 7: Beam loss distribution in the whole ring of MR 490 kW user operation with fast extraction. Left figure is the contour plot of the beam loss monitor (BLM) signals in time variation. Right figure is their accumulated signals in time. Both horizontal axes show the index number of the BLMs in the MR. The BLMs are set in low gain at the collimator section, while they are set in high gain in 8 times at the non-collimator section.

Upgrade Plan

We plan to make faster cycle from 2.48 s to 1.3 s to achieve 750 kW, and to 1.16 s to achieve 1.3 MW with 3.3 $\times 10^{14}$ ppp [16]. 80% of required number of protons for the 1.3 MW scenario were accelerated in 2.48 s cycle. Hardware upgrades are under construction [16, 17].

In the view of beam tunings, we expect linear increment of beam losses and residual doses corresponding the cycle time. To keep well-controlled residual activation, we are discussing new collimator scenario. Collimators having rotational jaw angle are partially adopted and they are effective to absorb beam halos [18]. Same type collimators will be added. Moreover, two stage collimator system is under discussion and some beam test was performed [19].

THE MR WITH SLOW EXTRACTION

The MR with slow extraction has been operated near the tune (22.30, 20.80), and use the third resonance line, nx = 22.33, during the extraction. The high extraction efficiency, 99.5%, has been achieved by the dynamic bump scheme, overlapping the outgoing arms of the separatrices at the electrostatic septum from the beginning to the end of slow extraction [20]. The spill regulation system, which consists of 3 different knobs: extraction quadrupoles, ripple quadrupoles and transverse RF, has enable good spill structure and its duty factor in 30 ~ 50% [20, 21]. The beam power has been increased steadily with keeping the beam quality. To extract more protons per pulse, following tunings has been taken, also. RF beam loading compensation is for debunching process [22]. Chromatic tuning before the extraction is to suppress the transverse instability. Longitudinal dipole oscillation was controlled [23] to suppress the electron cloud and instability [24]. For further power up to 51 kW (5.5×10^{13} protons per pulse), cycle time was changed from 5.52 s to 5.20 s with keeping spill length 2 s, high efficiency 99.5% (see Fig. 8 and 9). Beam loss are well localized at the septum area during the slow extraction at the flat top (see Fig. 10).

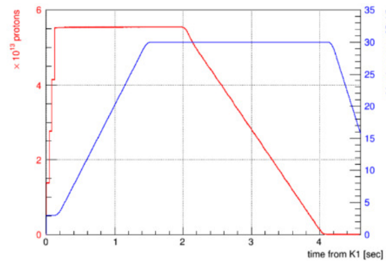

Figure 8: DCCT (red line) and kinetic energy pattern (blue line) of MR 51 kW with slow extraction in 5.20 s cycle.

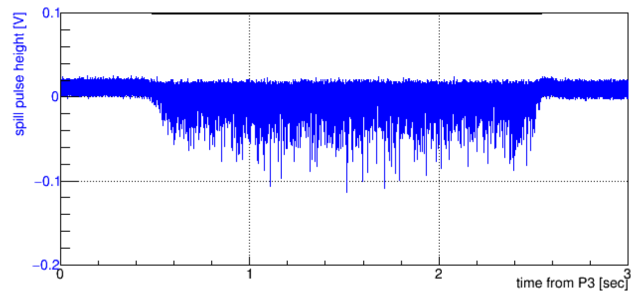

Figure 9: The spill structure of MR 51 kW user operation with slow extraction. The spill length was kept 2 s.

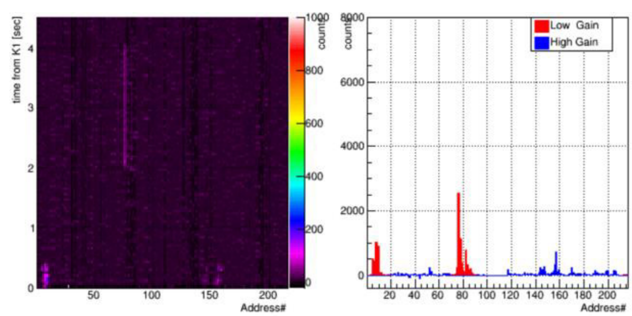

Figure 10: Beam loss distribution in the whole ring of MR 51 kW user operation with slow extraction. Left figure is the contour plot of the beam loss monitor (BLM) signals in time variation. Right figure is their accumulated signals in time. Both horizontal axes show the index number of the BLMs in the MR. The BLMs are set in low gain at the collimator section and the slow extraction section, while high gain in other section.

SUMMARY

In the RCS, 1 MW acceleration was successfully tested with minimum beam loss. The RCS enables high intensity beam operation for both the MLF and the MR with well suppressed beam loss, though each operation has different requirement. The MR with fast extraction achieved stable 490 kW user operation. Changing operation point was one of big keys to increase beam power. The MR upgrade is also planned with preparing faster cycle (from 2.48 s to ~1.3 s and 1.16 s). The MR with slow extraction achieved 51 kW user operation with > 99.5% efficiency. Beam power was successfully increased with faster cycle from 5.52 s to 5.20 s.

ISBN: 978-3-95450-184-7 doi:10.18429/JACoW-IPAC2018-THYGBF1

REFERENCES

[1] T. Koseki *et al.*, Prog. Theor. Exp. Phys. 2012 1: 02B004 (2012).
[2] H. Hotchi *et al.*, Phys. Rev. Accel. Beams **20**, 060402 (2017).
[3] H. Hotchi *et al.*, Phys. Rev. ST Accel. Beams **15**, 040402 (2012).
[4] H. Hotchi *et al.*, in *Proc. of IPAC2018*, TUPAL018, Vancouver, Canada, 2018.
[5] H. Hotchi *et al.*, in *Proc. of IPAC2016*, Busan, Korea, 2016, pp. 592 - 594.
[6] K. Ohmi *et al.*, *Proc. of HB2014*, East-Lansing, MI, USA, 2014, WEO2LR03, pp. 259 - 266.
[7] S. Igarashi, *et al*., *Proc. of HB2016*, Malmo, Sweden, 2016, MOAM6P60, pp. 21-26.
[8] Y. Hashimoto *et al.*, *Proc. of HB2014*, East-Lansing, MI, USA, 2014, TUO2AB04, pp. 187 - 191.
[9] K. Kurimoto and K. Nakamura, NIM A Vol. **840**, 160 (2016).
[10] T. Sugimoto *et al.*, in *Proc. IPAC2014*, Dresden, Germany, 2014, MOPME069, pp. 526-528.
[11] T. Sugimoto *et al.,* in *Proc. IPAC2016*, Busan, Korea, May 2016, THPMW021, pp. 35883590.
[12] Y. Kurimoto *et al.*, in *Proc. DIPAC2011*, Hamburg, Germany, 2011, paper TUPD74, pp. 482-484.
[13] K. Nakamura *et al.*, in *Proc. IPAC2014*, Dresden, Germany, 2014, paper THOAA03, pp. 2786-2788.
[14] A. Kobayashi *et al.*, US-Japan Meeting on Acc. for neutrino beams, Batavia, IL, USA, Mar. 2018.
[15] A. Chao *et al.*, Phys. Rev. ST Accel. Beams **5**, 111001 (2002).
[16] T. Koseki *et al.*, in *Proc. of IPAC2018*, TUPAC005, Vancouver, Canada, 2018.
[17] K. Hasegawa *et al.*, in *Proc. of IPAC2018*, TUPAL017, Vancouver, Canada, 2018.
[18] M. Shirakata *et al.*, *Proc. of HB2016*, Malmo, Sweden, 2016, THAM4Y01.
[19] Y. Sato *et al.*, *Proc. of PASJ2017*, Sapporo, Japan, 2017, WEOL03.
[20] M. Tomizawa *et al.*, *Proc. of IPAC2012*, New Orleans, USA, MOPPD051, pp. 481-483, 2012.
[21] A. Schnase *et al.*, *Proc. of IPAC2010*, Kyoto, Japan, pp. 1446-1448, 2010.
[22] F. Tamura *et al.*, Phys. Rev. ST Accel. Beams, **16** 051002 (2013).
[23] M. Tomizawa *et al.*, *Proc. of PASJ2016*, Chiba, Japan, MOOM05, pp. 70-74.
[24] B. Yee-Rendon *et al.*, *Proc. of IPAC2017*, Copenhagen, Denmark, pp. 4436-4438, 2017.